The Slip-Pad: A Haptic Display Using Interleaved Belts to Simulate Lateral and Rotational Slip

Colin Ho[1*], Jonathan Kim[2*], Sachin Patil[3], Ken Goldberg[4]

***Abstract*— We introduce a novel haptic display designed to reproduce the sensation of both lateral and rotational slip on a user's fingertip. The device simulates three-degrees-of-freedom of slip by actuating four interleaved tactile belts on which the user's finger rests. We present the specifications for the device, the mechanical design considerations, and initial evaluation experiments. We conducted experiments on user discrimination of tangential lateral and rotational slip. Initial results from our preliminary experiments suggest the device design has potential to simulate both tangential lateral and rotational slip. Source files: `https://github.com/Slip-Pad`.**

I. Introduction

Research suggests that virtual reality and teleoperated systems benefit from accurate and responsive haptic representations [1]. The ability to display slip to a user's fingers could enhance precision grasps and manipulations within the virtual environment.

Slip contact forces, which are vital for grasp stability, include three primary modes of interaction between the object and fingertip: lateral (two dimensions in the plane of contact), normal (one dimension along the normal vector of the plane of contact) and rotational (one dimension consisting of rotation about the point of contact between the object and fingertip). Most prior haptic slip devices have the capability of addressing only one mode.

We present the design, implementation, and initial evaluation of a novel device for rendering lateral and rotational tangential haptic slips. Our device consists of an omnidirectional treadmill with two orthogonal pairs of miniature tactile belts interleaved with one another.

We postulate that this device could be used in operations demanding precise grasp control, like telerobotic laparoscopic surgical manipulations of delicate and slippery tissues.

To the best of our knowledge, this is the first device designed to render both lateral and rotational slips.

[1]Colin Ho is a PhD student in the Department of Mechanical Engineering, University of California, Berkeley, CA 94704, USA `colinho@berkeley.edu`

[2]Jonathan Kim is an undergraduate student in the Department of Electrical Engineering and Computer Science, University of California, Berkeley `jonkim93@berkeley.edu`

[3]Sachin Patil is a postdoctoral researcher and Executive Director of Cal-MR at the University of California, Berkeley `sachinpatil@berkeley.edu`

[4]Ken Goldberg is a professor in the Department of Industrial Engineering and Operations Research, University of California, Berkeley `goldberg@berkeley.edu`

*These two authors contributed equally to the work.

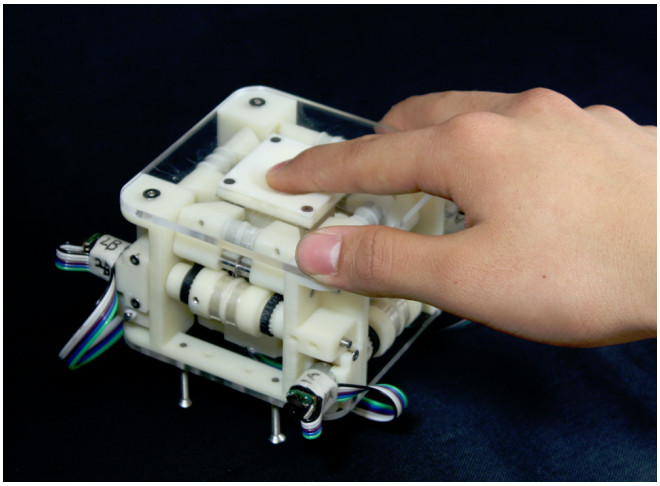

Fig. 1: A user's finger resting on our haptic slip device, demonstrating usage of the device and its scale. The device uses a pattern of four interleaving tactile belts sliding against a user's fingertip in order to communicate lateral and rotational slips. Preliminary evaluation experiments suggest the device's potential to reliably communicate lateral and rotational slip information.

II. Related Work

A. Principles of Touch and Grasping

Prior research has characterized how grasp stability is dependent on somatosensory input, such as displacements at the skin-object interface [2], [3]. For example, Nowak et al. showed that individuals with missing sensory feedback apply greater than necessary grip force when grasping and manipulating objects [2]. Moreover, individuals completing a grasp and lift task with slip sensory feedback impaired by anesthetics would initially fail to lift slippery objects [3]. The texture of objects plays an important role in slip speed perception of objects, as explored by Salada et al. [4]. Kinoshita et al. explored the effects of tangential torques on the control of grip forces when performing precision grips, and found "that the minimum normal force required to prevent slip, slip force, increases with tangential torque" [5]. Kinoshita et al. also wrote in their work that during grasps, "normal force appears to be constrained to increase and decrease in parallel with changes in tangential torque," an observation which suggests the vital role that tangential torque plays in helping modulate and adapt a human's grasp on a given object [5]. They concluded that when controlling normal force, "people take into account, in a precise fashion, the slip force reflecting both tangential force and tangential torque and their interaction as well as the current frictional condition in the object-digit interface."

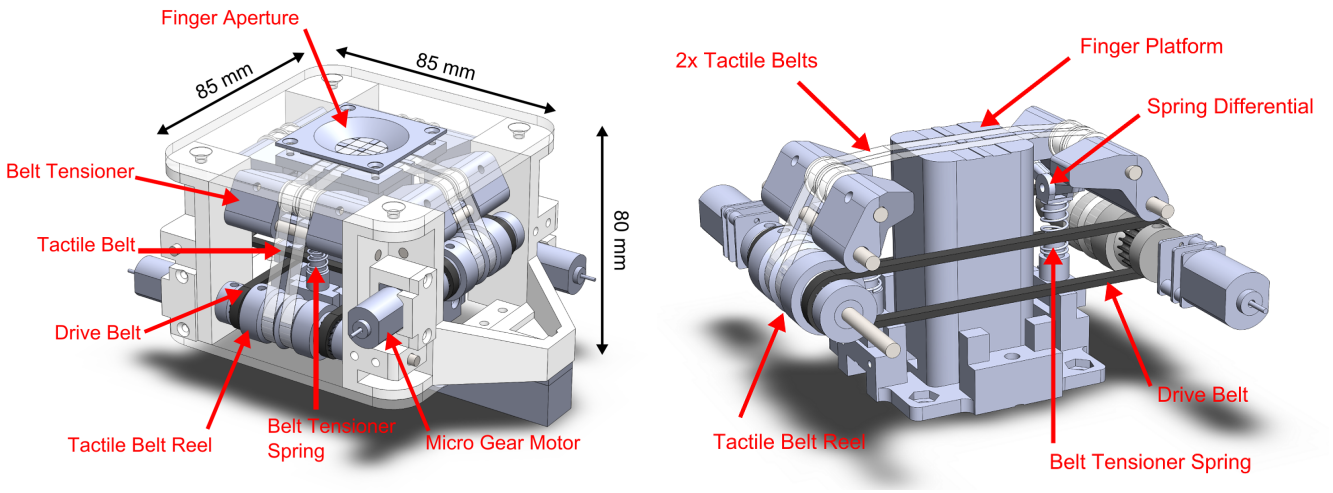

(a) Whole device

(b) Cutaway view of a single set of belts

Fig. 2: Diagram of haptic slip device dimensions and primary components. The device is driven by four independently actuated micro-motors. Each motor drives a tactile belt that runs over the top surface of the device, which is covered by an aperture designed to constrain the user's finger to remain on the area of actuation.

Additionally, Howe et al. proposed that a "function of torsion and shear magnitudes will adequately predict the onset of slip in many tasks" [6]. These results point to the vital role of lateral and torque slip sensory feedback in human grasping, tactile interaction, and exploration. Thus it is evident that accurate haptic rendering of slip forces would greatly benefit virtual reality and telerobotic operation applications.

For example, in the context of laparoscopic surgery, van der Putten et al. demonstrated that slip and vibro-tactile haptic feedback greatly aided participants' ability to modulate their pinch force to remain within required limits, and even found that approximately one-third of participants became dependent on the augmented feedback provided by their system [7].

B. Related Haptic Feedback Devices

Many researchers have developed devices to render slip forces to a human's fingertips. The devices surveyed fall into at least three separate categories: array-based, tactor-based, and ball-based.

One instance of an array-based device is the one developed by Wang and Hayward; they implemented a tactile transducer in the form of an array of piezoelectric actuators which would reproduce skin deformations on the user's fingertips to reproduce texture sensations but not slip sensations [8].

An example of a tactor-based device is the device developed by Gleeson, Horschel, and Provancher, who investigated the use of a skin stretch device as a means to haptically communicate directional information, as well as increase perception of friction, to a user [9]. Their device was composed of a rubber cylinder pressed against the user's fingertip and moved at constant speed to stretch the skin of the fingertip. Another example of a tactor-based device is that developed by Quek et al. [10]. Quek's device has three degrees of freedom and uses three constrained tactors interacting with three separate fingertips to render tangential skin stretch and normal skin deformation, but is unable to render lateral or rotational slips.

Webster and Okamura developed a ball-based device for rendering continuous sliding contacts in two dimensions to a user's fingertip in the form of a ball actuated by two orthogonal motors and demonstrated its usefulness in improving user performance in modulating applied force in virtual reality tasks [11]. Tsagarakis et al. developed a device they termed the "Slip Aesthesis", which used two miniature motors driving rotating cylinders in a V-shaped configuration to render sensations of relative lateral motion directly to the user's fingertip [12].

While these previous approaches are able to render only one of the *modes of slip* discussed in the introduction, our device is unique from previous approaches in its ability to display rotational slip. As demonstrated by Kinoshita, being able to render the rotational component improves a user's ability to perform stable grasps in both virtual and telerobotic environments.

III. DEVICE DESIGN

The device, as depicted in Fig. 1 and Fig. 2, consists of four interleaved plastic belts that are positioned underneath the fingertip. The plastic belts are split into pairs of belts that run parallel to one another. The pairs of belts run orthogonal to each other. The user places a finger on top of the belts through an aperture at the top of the device. The belts are then actuated, creating the desired relative lateral and/or rotational motion between the fingertip and the device. The belts are supported by a finger support from below, so the belts do not deflect under finger pressure.

A. Principle of Operation

The device is able to simulate both lateral and rotational slips by utilizing a system of four independently actuated tactile belts. The lateral slips can be rendered by the relative motion of the pairs of orthogonal belts with respect to one

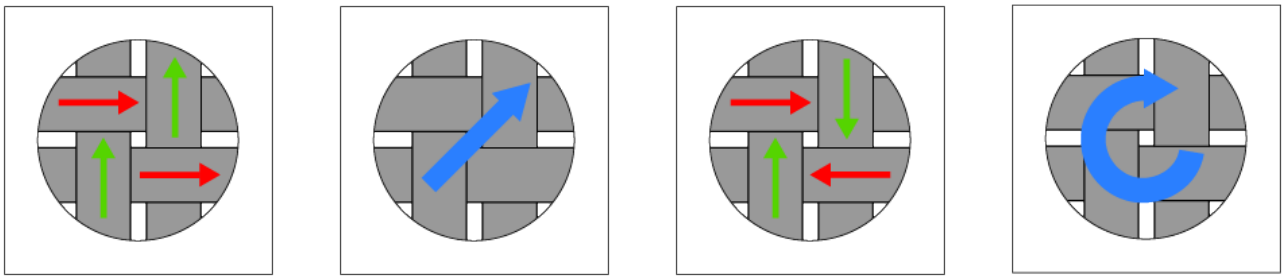

(a) Lateral: Motions of each belt **(b) Lateral:** Equivalent vector motion **(c) Rotation:** Motions of each belt **(d) Rotation:** Equivalent rotation

Fig. 3: This figure illustrates the principle of how the interleaved belts generate slip forces in both the lateral and rotational slip modes.

another. By mixing the magnitude and direction of these orthogonal motions, any lateral direction of slip can be rendered, as shown in Fig. 3.a and Fig. 3.b.

Rotational slips are rendered by having each belt move clockwise or counterclockwise with respect to the center of the aperture. The resulting motion of each pair of parallel belts moving in opposition to one another generates a rotational motion around the center of the aperture, as shown in the Fig. 3.c and Fig. 3.d.

Lateral and rotational motions can be combined by summing the motions together to provide a total of 3 dimensions of freedom (x, y, and rotation) in the plane of the actuating surface.

B. Psychophysical Basis and Performance Requirements

The required maximum slip speed was chosen based on the estimated maximum fingertip velocity while conducting dexterous manipulation tasks. The driving torque required was determined by estimating the maximum amount of normal force that would be exerted by the user. A normal force value of 10 Newtons was estimated by applying a series of varying intensity pinch presses to a load cell. Motor torque is calculated by estimating the frictional force that must be overcome. From [13], we get an estimated static friction coefficient of $\mu_{static} = 0.6$ for finger skin contact with PE plastic, which provides a motor torque requirement of 0.43 kg-cm (given an estimated belt reel diameter of 14 mm). A motor speed requirement of 410 rpm can be calculated from the maximum desired slip speed of 300 mm/s, given an estimated belt reel diameter of 14 mm.

The final important specification is slip distance resolution. The distance of 0.2 mm is derived from skin stretch perceptual experiments from Gleeson et al. that found that value to be close to the bottom threshold for direction detection accuracy. The required angular positioning resolution of the motors can be determined with an estimated belt reel diameter of 14 mm. The desired angular resolution of the motors was calculated to be 1.6°.

Based on these considerations, we derived the following high-level design specifications:

- Max slip speed of at least 300 mm/s
- Slip distance resolution of at least 0.2 mm [14]

Additionally, a fingertip aperture is needed to ensure that lateral motions are precisely translated to finger skin surface without hysteresis. From [15] and [11], a fingertip aperture with a diameter of 15 mm was selected.

C. Design of Haptic Device

The design of the haptic slip device centers around the four tactile belts that can be seen in Fig. 2. The tactile belts were chosen to be non-continuous, in order to enable the testing of various tactile textures. Initial experiments with smooth tactile belt material led us to hypothesize the need for textured tactile belts, which necessitated the use of non-continuous belt material. In order to actuate a non-continuous belt, the reels on either side of the belt need to be driven synchronously. A miniature drive belt and pulley system was designed to accomplish this. As seen in Fig. 2, these drive belts couple each pair of reels to drive a single tactile belt. GT2 profile 2 mm pitch belts were chosen for their ability to accurately translate linear motions without backlash.

One issue introduced by the use of non-continuous belt loops was that as the reels rotated synchronously, transferring belt from one to another, one reel would increase in diameter while the other would decrease. This results in a change in belt distance between one reel to the other, creating slack in the tactile belt. This was resolved by creating independent spring-loaded belt tensioners for each tactile belt, to ensure constant belt tension is maintained for consistent slip motions. These tensioners were designed to be able to compensate for up to 6 mm of belt slack, and they utilize a lever differential to evenly distribute force from a single tension spring to two different parallel belts (Fig.2.b).

The final design incorporates four 30:1 micro gear-motors that drive each of the tactile belt reel assemblies. The motors chosen are capable of 1.1 kg-cm of torque, and a maximum no-load shaft speed of 600 rpm, which translates to a theoretical maximum lateral slip speed of 430 mm/s. The actual maximum lateral slip speed is closer to 300 mm/s due to friction and loading on the system. Each motor has a 30:1 gearbox reduction and a 12-count rotary encoder on the motor itself, which gives a theoretical minimum of 0.05 mm of slip distance resolution. However, manufacturing and assembly tolerances of the gearbox introduce a certain amount of angular backlash which results in about 0.2 mm of linear backlash of the tactile belts. Since the motors are capable of variable output, the slip speed rendered by the device is controllable and can be varied.

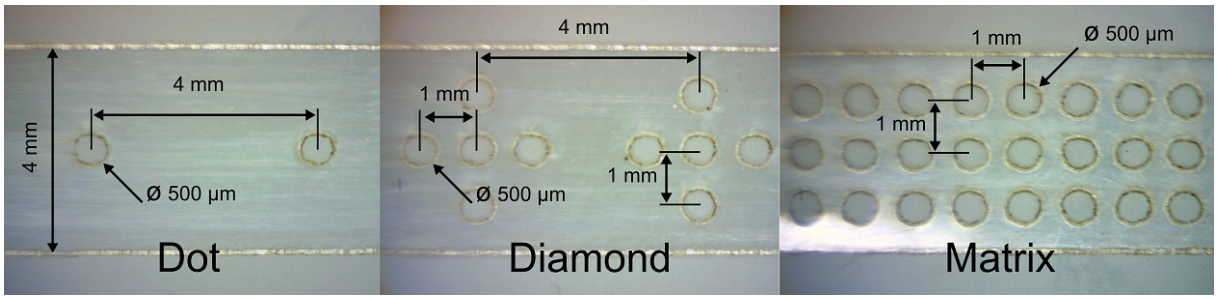

Fig. 4: Tactile belt patterns and dimensions. In order to improve user perception of slip distance and velocity, we laser-cut various patterns (adapted from neurophysiological literature on tactile perception) into the tactile belts, to provide surface microgeometries for the user's finger to slide against when using our belt-driven device.

The tactile belts are positioned 3 mm away from the center-point of the aperture measured from the tactile belt's centerline. With a maximum lateral slip speed of 430 mm/s, the theoretical maximum angular velocity is $12,900°$/s, or approximately 36 revolutions/s.

D. Tactile Belt Design

The unique interwoven tactile belt pattern is key to enabling both rotational and lateral slip motions. We chose to pattern the tactile belts with different textures after finding through initial experiments that smooth-surface tactile belts seemed to give ambiguous information about direction of angled motion, a result supported by research done by Salada and Srinivasan, who found that the textural features of a surface are important for a human to determine slip speed [4], [16]. For this prototype we chose to use finite lengths of material (700 mm in length) attached at either end to the device reels, with four different textures laser-engraved in 125 mm segments along the length of the belt. We chose to use finite lengths of material because continuous loops (which, with the same form factor, would have had a length of approximately 170 mm) would have given much less space to engrave textures, and would have forced us to dedicate individual belt sets to each pattern.

The patterns engraved on the belts were selected by referencing various papers in the literature about human tactile detection of microgeometries on otherwise smooth surfaces. The first pattern was chosen to be a smooth surface, to serve as a control against the other textural patterns. The second pattern was chosen to be a line of dots 500 μm in diameter, with 4 mm of distance between each dot. This pattern was designed and selected by referencing Srinivasan's paper on how different microgeometries activate certain specific neural fibers leading to the perception of slip [16]. One of the patterns that Srinivasan investigated was a single raised dot; we extended this idea to design a chain of dots in order to extend the perception of slip over a distance. The third pattern was again based on a pattern investigated by Srinivasan; the pattern we implemented was a matrix of dots spaced 1 mm along the length of the tape, and spaced 1 mm along the width of the tape. The fourth and final pattern was based on a diamond-shaped pattern investigated by Darian-Smith, which was found to activate the Pacinian nerve fibers, which are associated with perceptions of slip [17].

Since the tactile belts can only be driven for a finite distance, it drives the need for a large slip rendering distance which in turn necessitates the use of thin belt materials. A Polyester (PET) plastic material of 50 μm was selected, since it was thin enough to allow for a relatively small diameter reel to actuate it, but strong enough to not plastically deform when slipping under strong finger presses. Sheets of this material were laser cut into thin 4 mm wide bands to create the tactile belts.

E. System Integration

The device's four motors are controlled by C++ code running on a 32-bit ARM-M4 microprocessor. The motors are commanded by passing packets over a USB serial connection to the microprocessor, which then sets motor speed and position using a proportional-integral-derivative (PID) controller.

In order to aid in conducting user studies, we developed a graphical user interface (GUI) in Java that allowed for easy adjustment of angle and speed values, as well as easy command of torque values. The GUI's backend would send messages over a serial connection to the microprocessor at a rate of 200 Hz; the low-level motor control code would then execute at a rate of 1 kHz. Thus, the latency of the device in response to different motor commands was on the order of 5 ms. According to Johansson and Westling in their study of precision grip forces exerted by humans, during adjustments of grip force balance in response to small short slips, the latency between slip and grip adjustment took around 60-80 ms [3]. Thus, the latency that resulted from differences between the GUI refresh rate and the microprocessor refresh rate should not be significant enough to interfere with the human's response time.

IV. Prototype Design Evaluation

We conducted preliminary device evaluation studies to test different tactile belt surfaces on the device and to guide design choices for future iterations of the device. We hypothesized that users would be able to discriminate between lateral slip angle directions simulated by the device, and recognize the direction of simulated rotational slip. We also hypothesized that the tactile belt texture will have an influence on the accuracy of slip lateral and rotational direction detection.

A. Angle Discrimination Evaluation

Thus for the first device experiment, we performed an angle discrimination test, similar to the one conducted by Webster and Okamura, in which users were asked to determine the direction of angular slip as rendered by the device [11]. The user was instructed to exert approximately force of 100g on the slip device, and was given a scale to practice applying a consistent 100g of force. The user was then seated at a table, with their dominant hand's index finger placed above the slip device. The user was first blindfolded and given headphones playing white noise to eliminate any other sensory information, and then they were presented with a random sequence of 20 different slip angles at speeds of 10 cm/s, ranging from -50 to 50° in 5 degree increments (with 0° being slip in the forward direction). This procedure was repeated for a total of four times, each time switching the belt texture in a randomized order. The user was allowed to feel each slip orientation for as long as they liked. The user was told to lift their finger between each slip angle trial in order to allow the device to respool. For each trial, the user was queried whether they felt that their finger was slipping forward or angled and which direction (left or right) if angled. Six users, three female and three male, all right-handed and ranging from ages 21 to 26, performed this experiment. The results from these initial experiments are presented in Fig. 6 on the bottom of this page.

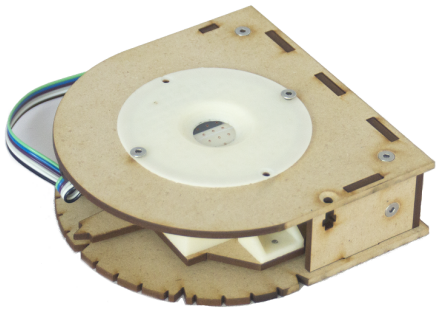

(a) The "control" lateral slip device used

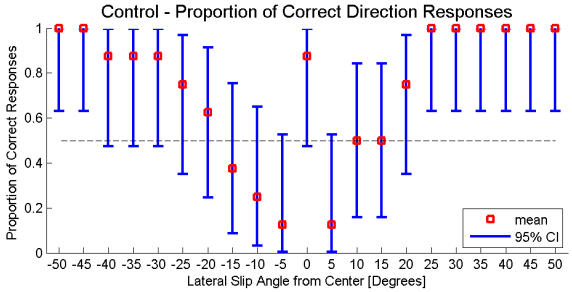

(b) The proportion of correct angle direction responses

Fig. 5: This figure displays the "control" device that was used, and the results of displaying an angled output and querying users' interpretation of the angle direction. The x-axis is the angle of lateral slip which the device simulates, and the y-axis is the proportion of correct responses when users were queried as to what direction the device was moving their finger (options were "left" for negative perceived angles, "right" for positive perceived angles, and "straight" for 0-degree perceived angles). The dotted line is the 0.5 proportion response threshold, and the error bars indicate the 95% binomial proportion confidence interval.

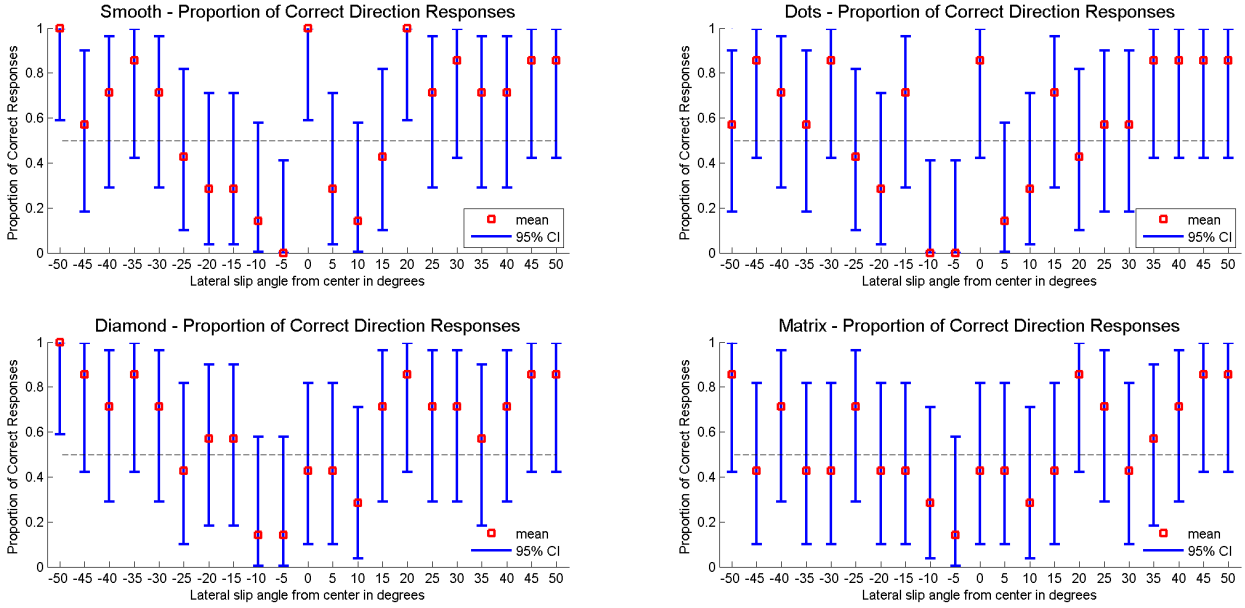

Fig. 6: This figure contains the preliminary results of the direction discrimination tests. The x-axis is the angle of lateral slip which the device simulates, and the y-axis is the proportion of correct responses when users were queried as to what direction the device was moving their finger (options were "left" for negative perceived angles, "right" for positive perceived angles, and "straight" for 0-degree perceived angles). The dotted line is the 0.5 proportion response threshold, and the error bars indicate the 95% binomial proportion confidence interval. Analysis of this data seems to indicate that users are better at discerning the direction of larger angle movements, which aligns with our hypothesis.

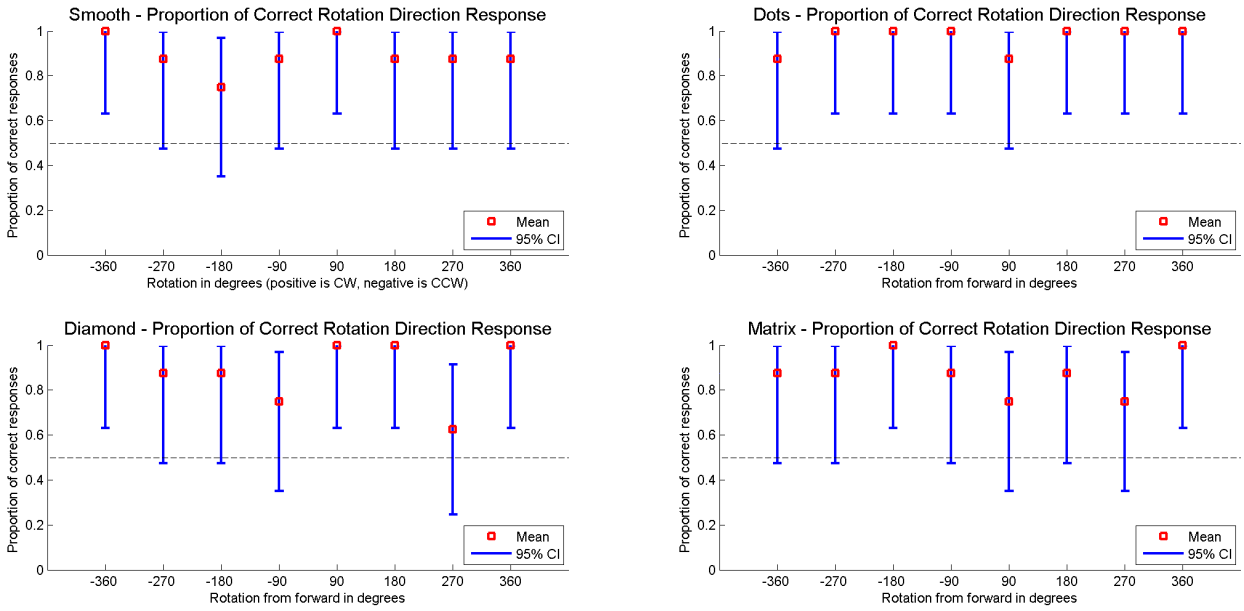

Fig. 7: This figure contains the preliminary results of the rotation discrimination tests. The x-axis is the degree of rotation which the device simulates, and the y-axis is the proportion of correct responses when users were queried as to what direction the device was slipping with respect to their finger (options were clockwise or counterclockwise). The dotted line is the 0.5 proportion response threshold, and the error bars indicate the 95% binomial proportion confidence interval. Analysis of this data seems to indicate that users are able to discriminate rotational slip directions, which aligns with our hypothesis.

B. Angle Discrimination Control Evaluation

We conducted a control device evaluation to get a baseline estimation of the angle at which users could detect angled slips. We built a "control" lateral slip device in order to provide comparison data for the experiments. The control device (depicted in Fig. 5.a), consists of a single motor driving a 20 mm wide tactile belt with a 4mm grid of evenly spaced dots. This single tactile belt functions as a single surface, in contrast to the interleaved belt surfaces of the Slip-Pad device design. The single tactile belt can be oriented from +90 to -90°, to simulate the full range of angled lateral slips. We conducted the same angle discrimination experiment, querying participants' responses (left, right, or straight) to a random sequence of 20 different slip angles ranging from -50° to 50° in 5° increments. Four users, three male and one female, all right-handed and ranging from ages 21 to 24, performed this experiment with two trials each resulting in 8 samples. The threshold at which approximately 50% of the users could detect the angle was 20°. The results from these control experiments are shown in Fig. 5.b. Our control evaluation, though not statistically significant, aligns with existing psychophysical slip angle discrimination experiments conducted by Webster and Okamura which found 20° to be the angle discrimination threshold [11]. Slight differences can be attributed to differing surface textures as shown by Salada et al., and the small sample size of this evaluation [4].

C. Rotation Discrimination Evaluation

The user was presented with a random sequence of 16 different actuations of the device, during each of which the device rendered a rotation through a randomized angular distance ranging from -360 to 360° (with -360° being a complete revolution in the counterclockwise direction, and 360° being a complete revolution in the clockwise direction) in increments of 90°. The user was then asked what direction they had perceived the rotation to be in (either clockwise or counterclockwise). This procedure was repeated for a total of four times, each time switching the belt texture in a randomized order. Four users, two female and two male, all right-handed and ranging from ages 21 to 24, performed this experiment. The results from these initial experiments are presented in Fig. 7 at the top of this page.

V. Discussion

Our preliminary user studies suggest that the dotted tactile belt pattern seemed to yield the best accuracy in user response for the rotation direction discrimination test. Additionally, the matrix tactile belt pattern seemed to be less effective than we had hypothesized; relatively speaking, users' accuracy on the angle discrimination tests with the matrix pattern seemed to be somewhat lower than the accuracy achieved with other patterns. The matrix and diamond patterns also seemed to yield a higher proportion of false positives during the angle discrimination test when the user was asked if the device output was angled or straight; users were more likely to respond to an angle of 0 with an "angled" response with these two textures than for the dotted and smooth textures. For the angle discrimination test, it does appear that the higher angle values are correlated with higher accuracy in perceived direction, though this seems less pronounced in the matrix pattern data. Since the sample size is so low, it is difficult to come to any strong conclusions about the data; however, the smooth and dotted

results appear to be correlated with the control results. The results of the rotational slip experiment also seem to point to very high levels of accuracy in discriminating direction of rotational slip outputs; however, it appears that the diamond and matrix patterns again are less effective than the dotted and smooth patterns. We hypothesize that the dotted texture outperformed the diamond and matrix textures because it provided regularly spaced, contrasting (smooth versus bump) tactile features, thus enabling the detection of slip distance.

During the angle discrimination test, some users indicated that for angled movements they perceived different speeds between belts parallel to each other. However, parallel belts were always driven at equal speeds. We hypothesize that this perception of differing speeds comes from the two-by-two interwoven pattern of the tactile belts; since each of the four belts makes contact at different quadrants on the finger pad (as can be seen in Fig. 3), the normal force applied to each quadrant may vary, thus causing variation in perceived friction force and thus speed. We plan on addressing this limitation in future iterations by doubling the number of tactile belts to create a four-by-four interwoven belt pattern.

VI. Future Work

In the experiments covered by this work, we commanded the belts to run at a constant speed; future experiments will include varying slip speed and measuring the effects on user perception with differing speeds.

For future iterations of the device, we plan on integrating a load cell into the device to allow for measurement of force exerted by the user's fingertip, and thus extend the device's capabilities to include measuring force input. Additionally, we plan on using continuous belts to help reduce the device size and to remove the need for regular respooling.

We also plan on investigating the concepts of skin stretch and normal deformation with future iterations of the device. The phenomenon of skin stretch is particularly vital when it comes to maintaining grasp stability in the absence of slip. Quek et al. found that the ability to render skin stretch and normal deformation through a haptic device greatly aided participants' ability to locate a contoured hole in a virtual surface [10]. Our device can easily be adapted to render these skin stretch forces, simply by using a belt material with a higher frictional coefficient, and by commanding smaller motions to the belts. Additionally, normal skin deformation rendering could be integrated by introducing actuated tactors patterned between the belts that can extend or withdraw depending on the amount of normal deformation desired.

VII. Conclusion

In this paper we present a novel haptic slip display capable of rendering both rotational and lateral slip forces. Our preliminary psychophysical studies suggest that the device has potential to convey both lateral and rotational slip. Further design improvements to the device include increasing the number of tactile belts to address issues of asymmetry, using continuous belts to allow for miniaturization, and integration with force sensing, skin deformation and deflection.

Acknowledgments

We would like to thank Allison Okamura and her lab for their feedback and insights.

References

[1] Blake Hannaford and Allison M. Okamura. Haptics. In Bruno Siciliano Prof and Oussama Khatib Prof, editors, *Springer Handbook of Robotics*, pages 719–739. Springer Berlin Heidelberg, January 2008.

[2] Dennis A. Nowak, Stefan Glasauer, and Joachim Hermsdrfer. How predictive is grip force control in the complete absence of somatosensory feedback? *Brain*, 127(1):182–192, January 2004.

[3] R. S. Johansson and G. Westling. Roles of glabrous skin receptors and sensorimotor memory in automatic control of precision grip when lifting rougher or more slippery objects. *Experimental Brain Research*, 56(3):550–564, October 1984.

[4] M. Salada, P. Vishton, J.E. Colgate, and E. Frankel. Two experiments on the perception of slip at the fingertip. In *12th International Symposium on Haptic Interfaces for Virtual Environment and Teleoperator Systems, 2004. HAPTICS '04. Proceedings*, pages 146–153, March 2004.

[5] Hiroshi Kinoshita, Lars Bckstrm, J. Randall Flanagan, and Roland S. Johansson. Tangential Torque Effects on the Control of Grip Forces When Holding Objects With a Precision Grip. *Journal of Neurophysiology*, 78(3):1619–1630, September 1997.

[6] R.D. Howe, Imin Kao, and M.R. Cutkosky. The sliding of robot fingers under combined torsion and shear loading. In , *1988 IEEE International Conference on Robotics and Automation, 1988. Proceedings*, pages 103–105 vol.1, April 1988.

[7] E.P.W. van der Putten, J.J. van den Dobbelsteen, R.H.M. Goossens, J.J. Jakimowicz, and J. Dankelman. The Effect of Augmented Feedback on Grasp Force in Laparoscopic Grasp Control. *IEEE Transactions on Haptics*, 3(4):280–291, October 2010.

[8] Qi Wang and V. Hayward. Compact, Portable, Modular, High-performance, Distributed Tactile Transducer Device Based on Lateral Skin Deformation. In *2006 14th Symposium on Haptic Interfaces for Virtual Environment and Teleoperator Systems*, pages 67–72, March 2006.

[9] B.T. Gleeson, S.K. Horschel, and W.R. Provancher. Communication of direction through lateral skin stretch at the fingertip. In *EuroHaptics conference, 2009 and Symposium on Haptic Interfaces for Virtual Environment and Teleoperator Systems. World Haptics 2009. Third Joint*, pages 172–177, March 2009.

[10] Z.F. Quek, S.B. Schorr, I. Nisky, W.R. Provancher, and A.M. Okamura. Sensory substitution using 3-degree-of-freedom tangential and normal skin deformation feedback. In *2014 IEEE Haptics Symposium (HAPTICS)*, pages 27–33, February 2014.

[11] Robert J. Webster, III, Todd E. Murphy, Lawton N. Verner, and Allison M. Okamura. A Novel Two-dimensional Tactile Slip Display: Design, Kinematics and Perceptual Experiments. *ACM Trans. Appl. Percept.*, 2(2):150–165, April 2005.

[12] N.G. Tsagarakis, T. Horne, and D.G. Caldwell. SLIP AESTHEASIS: a portable 2d slip/skin stretch display for the fingertip. In *Eurohaptics Conference, 2005 and Symposium on Haptic Interfaces for Virtual Environment and Teleoperator Systems, 2005. World Haptics 2005. First Joint*, pages 214–219, March 2005.

[13] N.K. Veijgen, M.A. Masen, and E. van der Heide. Relating friction on the human skin to the hydration and temperature of the skin. *Tribology Letters*, 49(1):251–262, 2013.

[14] B.T. Gleeson, S.K. Horschel, and W.R. Provancher. Perception of direction for applied tangential skin displacement: effects of speed, displacement, and repetition. *IEEE Transactions on Haptics*, 3(3):177–188, July 2010.

[15] Mark A Salada, J Edward Colgate, Margaret V Lee, and Peter M Vishton. Validating a novel approach to rendering fingertip contact sensations. In *Haptic Interfaces for Virtual Environment and Teleoperator Systems, 2002. HAPTICS 2002. Proceedings. 10th Symposium on*, pages 217–224. IEEE, 2002.

[16] M. A. Srinivasan, J. M. Whitehouse, and R. H. LaMotte. Tactile detection of slip: surface microgeometry and peripheral neural codes. *Journal of Neurophysiology*, 63(6):1323–1332, June 1990.

[17] Ian Darian-Smith, Ian Davidson, and Kenneth O. Johnson. Peripheral neural representation of spatial dimensions of a textured surface moving across the monkey's finger pad. *The Journal of Physiology*, 309:135–146, December 1980.